THE JOURNAL OF PHYSICAL CHEMISTRY B

ARTICLE

pubs.acs.org/JPCB

The Effects of Protein Environment and Dispersion on the Formation of Ferric-Superoxide Species in *myo*-Inositol Oxygenase (MIOX): A Combined ONIOM(DFT:MM) and Energy Decomposition Analysis

Hajime Hirao*

Division of Chemistry and Biological Chemistry, School of Physical and Mathematical Sciences, Nanyang Technological University, 21 Nanyang Link, Singapore 637371

Supporting Information

ABSTRACT: The catalytic reaction of *myo*-inositol oxygenase, a nonheme diiron enzyme, is initiated by the binding of an O_2 molecule to the ferrous center of a mixed-valence Fe(II)Fe(III) intermediate. This generates a (superoxo)Fe(III)Fe(III) reactive species that abstracts a hydrogen atom from the *myo*-inositol substrate. To understand the effects of protein environment and intracluster dispersion on this O_2-binding process, we undertook a combined ONIOM(B3LYP:AMBER) and energy decomposition analysis. The interaction energy between the active site and the thousands of atoms present in the protein environment was decomposed into electrostatic, van der Waals (vdW) and polarization terms. These terms were further decomposed into contributions from individual amino acid residues. The dispersion effect, which is not adequately accounted for by the B3LYP method, was estimated in an empirical manner. The results show that the electrostatic, vdW, and polarization effects slightly enhance the O_2 binding process. The dispersion effect enhances O_2 binding more significantly than these effects. Despite these stabilizing effects, the entropy effect disfavors O_2 binding, making the process almost thermoneutral.

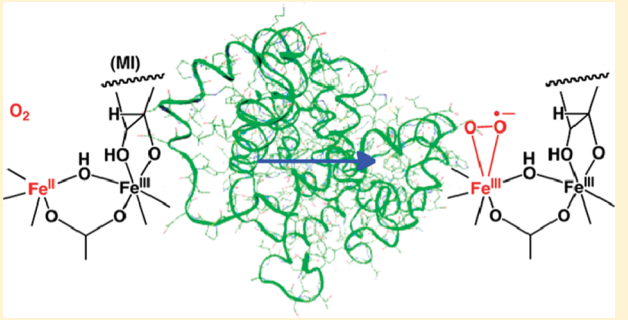

1. INTRODUCTION

Prominent catalytic functions of enzymes are controlled by various factors.[1] In the case of metalloenzymes involving a transition-metal ion, the formation of a highly reactive intermediate, which is typically made up of one or two metal ions and a few coordinating ligands, is one of the major factors that determine the catalytic proficiency of enzymes. The key characteristics of reactive intermediates of metalloenzymes have been mimicked to prepare bioinspired synthetic catalysts.[2−4] Another major factor that provides profound impacts on the catalytic activity of enzymes is the protein environmental effect. The selectivity and specificity of enzymatic reactions are usually remarkably finely tuned, which is largely because of the proper configuration and orientation of substrates that are judiciously regulated by the surrounding amino-acid residues. Moreover, the environmental effect often stabilizes the transition states of enzymatic reactions, thereby enhancing the reaction rate itself.[1a] As such, the bioinspired catalyst design in the future will also actively mimic and exploit the environmental effect of enzymes.[4] Such efforts will require precise identification of the individual factors that influence enzyme catalysis, and in this regard, computational approaches, such as hybrid quantum mechanical and molecular mechanical (QM/MM) methods,[5,6] should have useful roles to play.

This paper examines ways to analyze various factors influencing the enzyme activity using the ONIOM(QM:MM) method.[6]

Scheme 1. O_2 Binding Process in MIOX

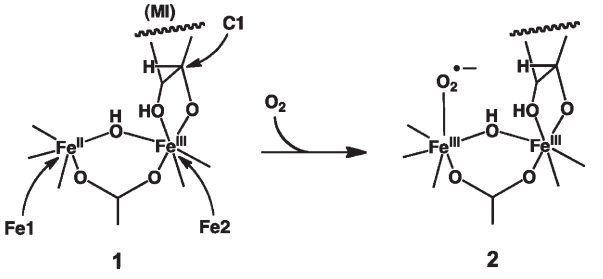

The enzyme that we shall study is *myo*-inositol oxygenase (MIOX), a dinuclear nonheme iron enzyme.[7,8] It has recently been shown that the catalytic cycle of MIOX involves the binding of an O_2 molecule to the ferrous center of a mixed-valence (superoxo)Fe(II)Fe(III) intermediate (**1**), to produce a (superoxo)Fe(III)Fe(III) intermediate (**2**) (Scheme 1). Intermediate **2** acts as a reactive species in abstracting a hydrogen atom from the C1 position of the *myo*-inositol (MI) substrate. This triggers the subsequent reactions, which eventually lead to the formation of

Received: June 18, 2011
Revised: August 14, 2011
Published: September 07, 2011

dx.doi.org/10.1021/jp2057173 | *J. Phys. Chem. B* 2011, 115, 11278–11285

D-glucuronate. Recently, ferric-superoxide (Fe(III)-$OO^{\bullet-}$) intermediates have attracted considerable attention in the area of bioinorganic chemistry,[2c,9] and MIOX is one of the representative iron enzymes of this type. Our recent computational study demonstrated that the ferric-superoxide intermediate **2** has the ability to abstract hydrogen from C1 of MI.[10]

The binding of O_2 to the metal sites of metalloenzymes has been identified as a challenging problem in computational chemistry.[11−16] It has been demonstrated that density functional theory (DFT) methods tend to estimate the process as being endergonic.[11,12] It has also been shown that the binding strength increases if QM/MM methods are employed, indicating that O_2 binding is enhanced by the protein environment.[13−16]

These previous studies prompted us to consider that the O_2 binding process of MIOX is intriguing as a subject of both bioinorganic chemistry and computational chemistry. In this paper, we investigate how the protein environment affects O_2 binding to the ferrous site in MIOX. This is done by the combined use of ONIOM(DFT:MM)[6] and energy decomposition analysis.[17] The latter approach is formulated so that it fits well with the ONIOM(DFT:AMBER) philosophy. Moreover, the decomposed energy terms are further decomposed into contributions from individual amino-acid residues. Such analysis aids our understanding of the intricate processes of enzymes.[18] On the theoretical side, another important issue in the treatment of metalloenzymes is that many of the conventional DFT methods do not adequately account for the dispersion effect.[19,20] Our previous study showed that the dispersion effect does not have a significant effect on the relative stability of structurally similar species.[10] However, the influence of the dispersion effect was slightly larger on the relative stability of two conformers for the ferrous state of soybean lipoxygenase-1 (2.8 kcal/mol).[21] This was because the two compared geometries were not very similar. More recently, Siegbahn et al. demonstrated that dispersion does have a significant effect on the properties of a variety of metalloenyzmes.[22] For example, for O_2 binding to the heme−Fe(II) system, the dispersion effect increased the O_2 binding energy by 7.7 kcal/mol. The Co−C bond dissociation energies of alkylcobalamins were shown to increase by >10 kcal/mol when an empirical dispersion correction was made. The large geometric and energetic impact of the dispersion correction on the H-abstraction step of cytochrome P450cam has also been reported by Lonsdale et al.[23] Therefore, in addition to the environmental effect, the effect of dispersion generally seems to play a critical role in metalloenzymes, and so it was examined for O_2 binding in MIOX by employing DFT-D as a higher-level calculation method for the ONIOM(QM:MM) approach.

2. METHODS

2.1. ONIOM Calculations. ONIOM(DFT:MM) calculations were performed using the Gaussian 09 program.[24] The ONIOM(QM:MM) energy is generally expressed as

$$E^{\mathrm{ONIOM}} = E^{\mathrm{real,\,MM}} + E^{\mathrm{model,\,QM}} - E^{\mathrm{model,\,MM}} \quad (1)$$

where "real" and "model" designate two systems defined for an entire enzyme, with the latter typically being smaller in size. QM and MM indicate that calculations are performed using QM/MM methods, respectively. The real and model systems for MIOX were defined in the same way as in our previous study.[10] The second term, namely, the QM energy for the model system, was calculated at the B3LYP/B1 level of theory,[25] where B1 stands for a combination of the SDD effective core potential basis set used for Fe and the 6-31G* basis set used for the rest of the QM atoms.[26] The 6-311+G(d,p) basis set (B2) was also used for single-point calculations. For MM calculations, the AMBER force field was used for the majority of atoms,[27] and the TIP3P model was used for water molecules.[28] The ONIOM(B3LYP:AMBER) method, defined in this way, is simply referred to as ONIOM in the following discussion.

Geometry optimization was performed with the mechanical embedding (ME) and electronic embedding (EE) schemes of ONIOM (i.e., ONIOM-ME and ONIOM-EE). For comparison, calculations on active-site models of **1** and **2** were also performed at the B3LYP/B1 level, with the C_β atoms of histidine and aspartate ligands fixed at the positions of the X-ray structure (PDB code 2HUO).[8a] The geometry of **2**, which was previously optimized with ONIOM-ME, was used as a starting point for this study.[10] Atomic charges assigned for the atoms in the model system were derived using the Merz−Kollman (MK) method.[29] When doing ONIOM-ME calculation, the charges of H-link atoms were always merged to the charge of the directly bound carbon (C_β) atoms, and H-link atoms were assumed to have zero charge. The total charges of the model and real systems were +1 and −10, respectively. ONIOM-ME geometry optimization of **2** was iterated with an updated set of MK charges for a newly optimized geometry, until the convergence of energy (<0.025 kcal/mol) was achieved. This required four iteration steps. After removing the O_2 molecule from the resultant geometry, the geometry of **1** was optimized in the same way. The final geometries of **1** and **2** were then subjected to ONIOM-EE geometry optimizations, in which the MM atomic charges for the model systems were identical to those used in the final iteration steps of ONIOM-ME optimizations.

To take into account the dispersion effect on the DFT energy and energy gradient, the empirical DFT-D formula proposed by Grimme was employed.[19] In this method, dispersion corrected energy ($E_{\mathrm{DFT\text{-}D}}$) is expressed as

$$E_{\mathrm{DFT\text{-}D}} = E_{\mathrm{DFT}} + E_{\mathrm{disp}} \quad (2)$$

where E_{DFT} is DFT energy and E_{disp} is dispersion energy:

$$E_{\mathrm{disp}} = -s_6 \sum_{i=1}^{N-1} \sum_{j=i+1}^{N} \frac{C_6^{ij}}{R_{ij}^6} f(R_{ij}) \quad (3)$$

where s_6 is a scale factor (1.05 for B3LYP), C_6^{ij} is a dispersion coefficient, R_{ij} is the distance between atoms i and j within the model system, f is a damping function, and N is the number of atoms in the model system. The current version of Gaussian 09 does not allow us to perform ONIOM(B3LYP-D:MM) (henceforth called ONIOM(D)) geometry optimization, but ONIOM(D) geometry optimization is possible if s_6 is reduced to 1.0. As this procedure covers a large part (>95%) of the E_{disp} value, the dispersion-corrected ONIOM geometry optimization was done in this way (i.e., ONIOM(D′)) in conjunction with the EE scheme (i.e., ONIOM(D′)-EE). Frequency calculations were also performed for entire enzymes (**1** and **2**) at the ONIOM(D′)-EE level to compute the free-energy correction (ΔG_{corr}) to the O_2 binding energy. For this purpose, the free energy of isolated O_2 was calculated at the B3LYP-D′/B1 level of theory. The intramolecular dispersion energy for O_2 was found to be so small that the addition of the dispersion correction (D′) did not change its geometry.

Scheme 2. Illustration of the Three Subsystems Employed

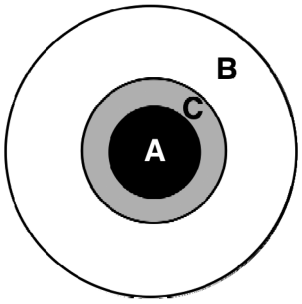

S = 1/2 spin states were assumed for both **1** and **2**. In both species, two high-spin iron centers are antiferromagnetically coupled, and in **2**, the superoxide moiety and the coordinating iron center are ferromagnetically coupled.[10] These states were approximated by broken-symmetry wave functions that the unrestricted formalism of DFT (UDFT) can produce. It was suggested in our previous study that a side-on coordination geometry having the S = 1/2 spin state is the ground state for **2**.[10] Therefore, the side-on geometry is used for this state throughout the analysis presented here. Molecular geometries were drawn with VMD.[30]

2.2. Energy Decomposition Analysis. For the entire enzyme system, we define three subsystems **A**, **B**, and **C** as illustrated in Scheme 2. Subsystem **A** is essentially the same as the model system but does not contain H-link atoms. Subsystem **B** consists of the majority of atoms outside of **A**. Subsystem **C** is a buffer region where all atoms up to three bonds away from the atoms in **A** at the covalent QM−MM boundary are included. The atomic charges for the atoms in **C** are zeroed when calculating the second term of eq 1 with ONIOM-EE.

For the defined subsystems, several interaction energy terms between the active site (**A**) and the protein environment (**B** and **C**) may be computed. The electrostatic interaction energy may be defined as

$$E_{\mathrm{es}} = \sum_{i \in \mathbf{A}} \sum_{j \in \mathbf{B},\mathbf{C}} (s_{ij}^{\mathrm{es}} q_i q_j / r_{ij}) \tag{4}$$

where q_i and q_j are point charges placed on atoms i and j in **A** and in **B** or **C**, respectively, and r_{ij} is the distance between them. The electrostatic energy between **A** and **C** is subjected to scaling depending on how many bonds are involved between the atoms. The scale factor s_{ij}^{es} is 0 if the two atoms are only one or two bonds away from each other. If there were three bonds between the atoms (1−4 interaction), the scale factor is 1/1.2.[27] It should be mentioned that, in calculating E_{es}, the charges of atoms in **A** (q_i) are obtained without allowing the wave function to polarize, namely, without placing the point charges of the surrounding atoms. The van der Waals (vdW) interaction energy is written in the 6−12 representation as

$$E_{\mathrm{vdW}} = \sum_{i \in \mathbf{A}} \sum_{j \in \mathbf{B},\mathbf{C}} s_{ij}^{\mathrm{vdW}} [A_{ij}/r_{ij}^{12} - B_{ij}/r_{ij}^{6}] \tag{5}$$

where the vdW scale factor s_{ij}^{vdW} is essentially the same as s_{ij}^{es} except in the 1−4 case (0.5 for vdW).[27] A_{ij} and B_{ij} are calculated as defined in AMBER,[27] from vdW parameters for each atom. The polarization energy is obtained from the ONIOM-ME and ONIOM-EE energies for the same geometry, viz.,

$$E_{\mathrm{pol}} = E^{\mathrm{ONIOM}}(\mathrm{EE}) - E^{\mathrm{ONIOM}}(\mathrm{ME}) \tag{6}$$

where the ONIOM energy values on the right-hand side were calculated with B3LYP/B1 gas-phase atomic charges (q_i) for this geometry assigned to the model system.

2.3. Further Decomposition into Residue Contributions. The above-defined energy terms can be further decomposed into the contributions from individual residues in region **B** or **C**. The electrostatic interaction between **A** and residue k (E_{es}^k) can be calculated by taking the interaction between i and $j \in k$ in eq 4:

$$E_{\mathrm{es}}^k = E_{\mathrm{es}}\{j \in k\} \tag{7}$$

where the curly brackets are used to explain the imposed condition. Likewise, the vdW interaction between **A** and residue k (E_{vdW}^k) can be calculated as

$$E_{\mathrm{vdW}}^k = E_{\mathrm{vdW}}\{j \in k\} \tag{8}$$

The polarization effect of residue k may be defined in two ways. In the first definition (E_{pol1}^k), ONIOM-EE and ONIOM-ME single-point calculations are done with the atomic charges for the residues other than k zeroed out, and the energy difference is taken:

$$\begin{aligned} E_{\mathrm{pol1}}^k &= E^{\mathrm{ONIOM}}(\mathrm{EE})\{q_{j \notin k} = 0\} - E^{\mathrm{ONIOM}}(\mathrm{ME})\{q_{j \notin k} = 0\} \\ &= E^{\mathrm{model,QM}}(\mathrm{EE})\{q_{j \notin k} = 0\} - E^{\mathrm{model,QM}}(\mathrm{ME}) - E_{\mathrm{es}}^k\{q_{j \in \mathrm{C}} = 0\} \end{aligned} \tag{9}$$

Alternatively, this quantity can be calculated by taking the difference between the QM energies in the ONIOM-EE and ONIOM-ME calculations, and then the resultant value is further subtracted by $E_{\mathrm{es}}^k\{q_{j \in \mathrm{C}} = 0\}$. $E_{\mathrm{es}}^k\{q_{j \in \mathrm{C}} = 0\}$ is essentially the same as E_{es}^k, but the charges in **C** are zeroed out. Thus, $E_{\mathrm{es}}^k\{q_{j \in \mathrm{C}} = 0\}$ is not equal to E_{es}^k if any atom in residue k belongs to **C**. It should be noted that $E^{\mathrm{model,QM}}(\mathrm{ME})$ does not change even if the atomic charges of the surrounding residues are altered. Therefore, E_{pol1}^k is more efficiently calculated by the latter procedure (transformed formula in eq 9), because one does not have to repeat ONIOM-ME calculations for all residues. Note that $E^{\mathrm{model,QM}}(\mathrm{EE})$ includes the effect of interactions between point charges and the wave function, but it does not include the self-interaction energies of point charges. A second definition for the residue-based polarization energy (E_{pol2}^k) may be given by

$$E_{\mathrm{pol2}}^k = E^{\mathrm{model,QM}}(\mathrm{EE}) - E^{\mathrm{model,QM}}(\mathrm{EE})\{q_{j \in k} = 0\} - E_{\mathrm{es}}^k\{q_{j \in \mathrm{C}} = 0\} \tag{10}$$

The first term in eq 10 is taken from the original ONIOM-EE calculation. The second term is the QM energy that is associated with the ONIOM-EE calculation in which the charges of the atoms (in **B** or **C**) for residue k are zeroed out. Because this zeroing also eliminates the electrostatic energy, the third term is required, as in eq 9. Many single-point calculations are necessary to obtain E_{pol1}^k and E_{pol2}^k; therefore, calculation of these quantities was done only for the ONIOM(D′)-EE geometry. It should be noted that, unlike the electrostatic and vdW interaction energies (E_{es} or E_{vdW}), the polarization energy (E_{pol}) is not an additive quantity with respect to the individual residue contributions. Therefore, the sum of the residue contributions (E_{pol1}^k or E_{pol2}^k) is not equal to E_{pol}.

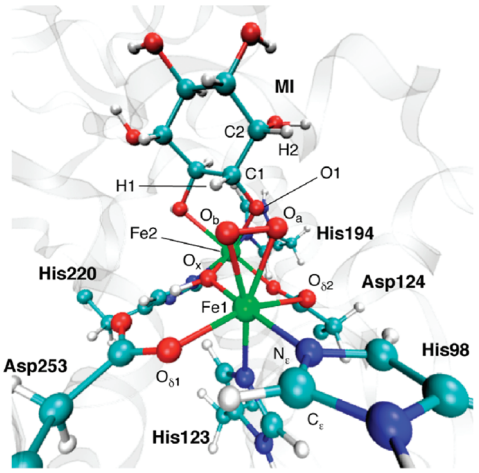

Figure 1. Active site of MIOX in the ferric-superoxide state (**2**).

Table 1. Key Bond Distances for 2 (in Å)

	r(Fe1−O_a)	r(Fe1−O_b)	r(O_a−O_b)
ONIOM-ME	2.188	2.167	1.284
ONIOM-EE	2.186	2.155	1.294
ONIOM(D′)-EE	2.171	2.133	1.297

3. RESULTS AND DISCUSSION

3.1. Geometric and Electronic Features of the Ferric-Superoxide Unit. To clearly evaluate the various effects on the geometry of the active-site cluster, the geometries of **1** and **2** were optimized by the ONIOM-ME, ONIOM-EE, and ONIOM(D′)-EE methods. It was shown by X-ray crystallography that an oxygen molecule should be bound to Fe1, while the substrate is bound to the other iron ion, Fe2 (see Scheme 1).[8] Figure 1 shows the active site of **2**, and Table 1 summarizes the key geometric parameters for the ferric-superoxide unit. At the ONIOM-ME level, the Fe−O_a and Fe−O_b distances, r(Fe−O_a) and r(Fe−O_b), were calculated to be 2.188 and 2.167 Å, respectively, and r(O_a−O_b) was 1.284 Å. These Fe−O distances were shortened by 0.002−0.012 Å when the polarization effect was introduced by ONIOM-EE. This is accompanied by a slight elongation of the O_a−O_b bond by 0.01 Å. The addition of the dispersion effect by ONIOM(D′)-EE further shortened the Fe−O distance by 0.015−0.022 Å, and elongated the O_a−O_b distance by 0.003 Å. These results therefore suggest that the polarization and dispersion effects enhance the binding of the O_2 molecule toward the Fe1 center.

Table 2 lists the spin population values (ρ) for the ferric-superoxide unit in the three different geometries. The values for Fe1 and the O_a−O_b part are 4.04 and 1.56, respectively. A pure superoxide unit should have a spin population value of 1.0, and the larger value obtained here is indicative of the incomplete charge transfer from the ferrous center to O_2, in the process of ferric-superoxide formation.[10] The ρ value for the O_2 unit was reduced to 1.48 (ONIOM-EE) and 1.46 (ONIOM(D′)-EE), indicating again that the polarization and dispersion effects enhance the O_2-binding process and the charge transfer from Fe(II) to O_2.

3.2. Stabilization Due to O_2 Binding. Table 3 summarizes the stabilization energy (ΔE) defined for the process

$$\mathbf{1} + {}^3O_2 \rightarrow \mathbf{2} \qquad (11)$$

Table 2. Key Atomic Spin Population Values for 2

	ρ(Fe1)	ρ(O_a)	ρ(O_b)
ONIOM-ME	4.04	0.79	0.77
ONIOM-EE	4.09	0.80	0.68
ONIOM(D′)-EE	4.09	0.79	0.67

Table 3. Summary of Stabilization Energy Values (ΔE in kcal/mol)

method	ΔE [kcal/mol][a]
B3LYP	−1.8[b]
ONIOM-ME	−3.1 (−1.5)[c]
ONIOM-EE	−3.5
ONIOM(D)-EE//ONIOM-EE	−10.6[d]
ONIOM(D)-EE//ONIOM(D′)-EE	−11.0[d] (−14.5)[e] [−7.6][f]
ONIOM(D)-EE//ONIOM(D′)-EE + ΔG_{corr}	−0.2 [d] (−3.8) [e] [3.2] [f]
ONIOM(D,B2)-EE//ONIOM(D′)-EE + ΔG_{corr}[g]	2.2 [d] (−0.9) [e] [5.3] [f]

[a] Stabilization due to O_2 binding. [b] The C_β atoms of the ligands are fixed at the positions of the X-ray structure (PDB code 2HUO).[8] [c] From the QM energy components of ONIOM. [d] B3LYP-D was used for the final energy evaluation. [e] B3LYP*-D was used for the final energy evaluation. [f] B3LYP(25)-D was used for the final energy evaluation. [g] B2 was used for the final energy evaluation.

At the B3LYP and ONIOM-ME levels, ΔE was calculated to be −1.8 and −3.1 kcal/mol, respectively, indicating that the O_2 binding is slightly exergonic. The magnitude of the ΔE value calculated by the QM-energy components of ONIOM-ME energies was 1.6 kcal/mol smaller (i.e., −1.5 kcal/mol) than that for ONIOM-ME, which means that O_2 binding is facilitated by the electrostatic and vdW effects that are included in ONIOM-ME calculations. It was found that ONIOM-EE geometry optimization slightly lowered the ΔE value (−3.5 kcal/mol). This is consistent with the observation in the previous section that the polarization effect enhances O_2 binding. Interestingly, the addition of the dispersion effect to the model systems in the ONIOM-EE-optimized geometries significantly lowered the ΔE value (to −10.6 kcal/mol), highlighting the importance of this effect. The ONIOM(D′)-EE geometry optimization did not change the ΔE value significantly. The B3LYP functional was used in this study simply because it has been the most popular functional for the study of metalloenzymes. There is no guarantee that B3LYP is sufficiently accurate for the description of the MIOX system. Unfortunately, the large molecular size does now allow us to apply accurate ab initio methods such as CCSD(T) or CASPT2 to the current system, and comparison of B3LYP with these methods, which may provide information about the accuracy of B3LYP, is not possible. Nevertheless, it should be meaningful to identify the functional dependence of the calculated O_2-binding energy. Siegbahn reported that the B3LYP* functional,[31] in which the amount of Hartree−Fock (HF) exchange in the B3LYP functional is reduced from 20% to 15%, gives 3.3 kcal/mol larger O_2 binding energy for an extradiol dioxygenase.[32] Consistent with this, the use of B3LYP*, instead of B3LYP, stabilized the O_2-bound state by 3.5 kcal/mol (Table 3). Conversely, when the amount of HF exchange was increased to 25% (designated here as B3LYP(25)), the O_2-bound state was destabilized by 3.4 kcal/mol (Table 3).

dx.doi.org/10.1021/jp2057173 |J. Phys. Chem. B 2011, 115, 11278–11285

Table 4. Summary of Decomposed Energy Values (in kcal/mol)

	E_{es}	E_{vdW}	E_{pol}	E_{disp} [b,c]
ONIOM-ME geom				
1	−322.9	−86.2	–	–
2	−322.8	−88.5	–	–
$\Delta E(\mathbf{2}-\mathbf{1})$ [a]	0.1	−2.3	–	–
ONIOM-EE geom				
1	−340.3	−75.3	−47.0	–
2	−341.0	−77.3	−47.9	–
$\Delta E(\mathbf{2}-\mathbf{1})$ [a]	−0.6	−2.0	−0.9	–
ONIOM(D′)-EE geom				
1	−340.4	−76.1	−46.7 (−90.8) [d] [−19.4] [e]	−97.2
2	−340.8	−78.2	−47.5 (−95.7) [d] [−15.9] [e]	−104.3
$\Delta E(\mathbf{2}-\mathbf{1})$ [a]	−0.5	−2.2	−0.7 (−4.9) [d] [3.6] [e]	−7.1

[a] Change in the energy term due to O_2 binding. [b] The contribution of the intramolecular dispersion energy of isolated O_2 is negligibly small. [c] Energies calculated with an s_6 value of 1.05 are presented. [d] From the sum of E^k_{pol1}. [e] From the sum of E^k_{pol2}.

It therefore appears that the amount of HF exchange has a great impact on the calculated binding energy. Free energy correction was found to weaken the O_2 binding by 10.8 kcal/mol, which is also consistent with previous studies on other enzymes.[13,16] As a result of the free-energy correction, the stabilization energy is calculated to be −0.2 and −3.8 kcal/mol with the B3LYP-D/B1 and B3LYP*-D/B1 methods. These results are consistent with the relatively rapid O_2 dissociation observed experimentally,[7c] whereas the B3LYP(25)-D/B1 method predicted O_2 binding to be slightly endergonic. When basis set B2 was used, the binding strength was weakened by a few kcal/mol. In this case, only B3LYP*-D predicted that O_2 binding should be exoergonic.

Let us now look into the environmental effect in more detail in light of the calculated decomposed energy terms (see Table 4). For the MIOX enzyme, the electrostatic energy term (E_{es}) was the largest in magnitude of all the terms considered. For example, for the ONIOM-ME geometry, E_{es} for **1** and **2** are −322.9 and −322.8 kcal/mol, respectively. Therefore, despite the large magnitudes of E_{es} values, the values are similar for **1** and **2**, and so the electrostatic effect does not make a significant contribution to O_2 binding. The magnitudes of E_{vdW} were much smaller than those of E_{es}. However, the stabilization effect due to the vdW interaction was larger for **2** than for **1** by 2.3 kcal/mol at the ONIOM-ME geometries. The vdW effect therefore plays a more important role in the enhancement of O_2 binding. The stabilizing effect of vdW intractions was also observed for O_2 binding in isopenicillin N synthase (IPNS), for which the vdW stabilization of the side-on geometry was calculated to be 4.4 kcal/mol.[16] It should be noted that the sum of ΔE_{es} and ΔE_{vdW} (−2.2 kcal/mol) is not exactly identical to the environmental stabilization effect observed in Table 3 for the ONIOM-ME geometry (−1.6 kcal/mol). This is because the present energy decomposition analysis ignores bonded energy terms due to stretching, bending, torsion, and out-of-plane torsion, as well as the nonbonded energy terms between atoms outside the model system, whereas the ONIOM-ME calculation includes these effects.

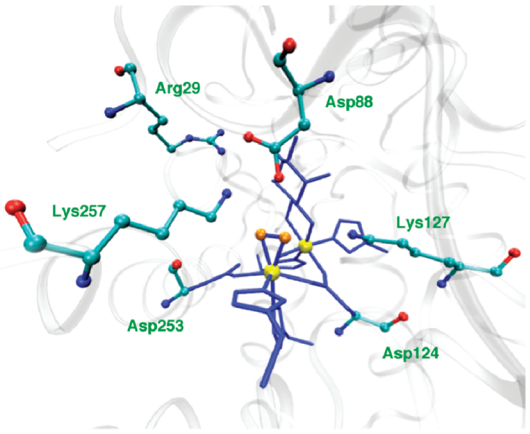

Figure 2. Key residues that have relatively large environmental effects on the ferric-superoxide formation process.

It turns out that the ONIOM-EE optimization changes the molecular geometry in a manner that decreases the E_{es} term by 17−18 kcal/mol and increases the E_{vdW} term by >10 kcal/mol. However, as far as the differences of these terms between **1** and **2** are concerned, these effects do not play significant roles. At this geometry, the magnitudes of E_{es}, E_{vdW}, and E_{pol} for **2** were larger than those for **1** by 0.6, 2.0, and 0.9 kcal/mol, respectively, meaning that all of these effects contribute to O_2 binding, even though the magnitudes are quite small.

Similar trends were observed for the ONIOM(D′)-EE geometry: the E_{es}, E_{vdW}, and E_{pol} terms contribute slightly to the O_2 binding here. However, the most important result is that the stabilization due to the dispersion effect is as large as 7.1 kcal/mol, which is much larger than the other three terms. For this geometry, E^k_{pol1} or E^k_{pol2} were also calculated, and the sums of contributions of all surrounding residues k (i.e., ΣE^k_{pol1} and ΣE^k_{pol2}, respectively) are also listed in Table 4. The ΣE^k_{pol1} values (−90.8 kcal/mol for **1** and −95.7 kcal/mol for **2**) are much larger in magnitude than the E_{pol} value, and the $|\Sigma E^k_{pol1}|$ value for **2** is 4.9 kcal/mol larger than that for **1**, compared with 0.7 kcal/mol for E_{pol}. In contrast, $|\Sigma E^k_{pol2}|$ for **2** is 3.6 kcal/mol smaller than that for **1**. Thus, although E^k_{pol1} or E^k_{pol2} may be useful for gaining insight into the polarization effect of individual residues, the sum of these quantities may not be considered to be useful.

3.3. Further Decomposition of the Interaction Energy. Equations 7−10 are now used to inspect how individual amino acid residues affect the O_2-binding process. The ONIOM(D′)-EE geometry was used for this purpose. A few residues in the vicinity of the active site were found to give relatively large values to E^k_{es}, E^k_{vdW}, or E^k_{pol} (Figure 2). Figure 3 plots the contribution of each residue to the electrostatic, vdW, and polarization interaction energies. Regarding the electrostatic interaction energy, Lys257 plays the most important role, stabilizing the O_2-bound state by −7.6 kcal/mol (Figure 3a). However, adjacent Asp88 has an adverse effect, which electrostatically destabilizes **2** by 5.9 kcal/mol. The destabilizing effect of Asp88 is attributed to the repulsion between the carboxylate oxygen atoms of Asp88 and the superoxide moiety. Other contributions were very small except for those of Arg29 (−1.0 kcal/mol), Asp124 (+1.2 kcal/mol), and Asp253 (+1.3 kcal/mol). No residue stabilized or destabilized the O_2 binding by >2 kcal/mol through vdW interactions (Figure 3b). The largest contributions are from Asp88 (−0.6 kcal/mol), Lys127 (−0.6 kcal/mol), and Lys257

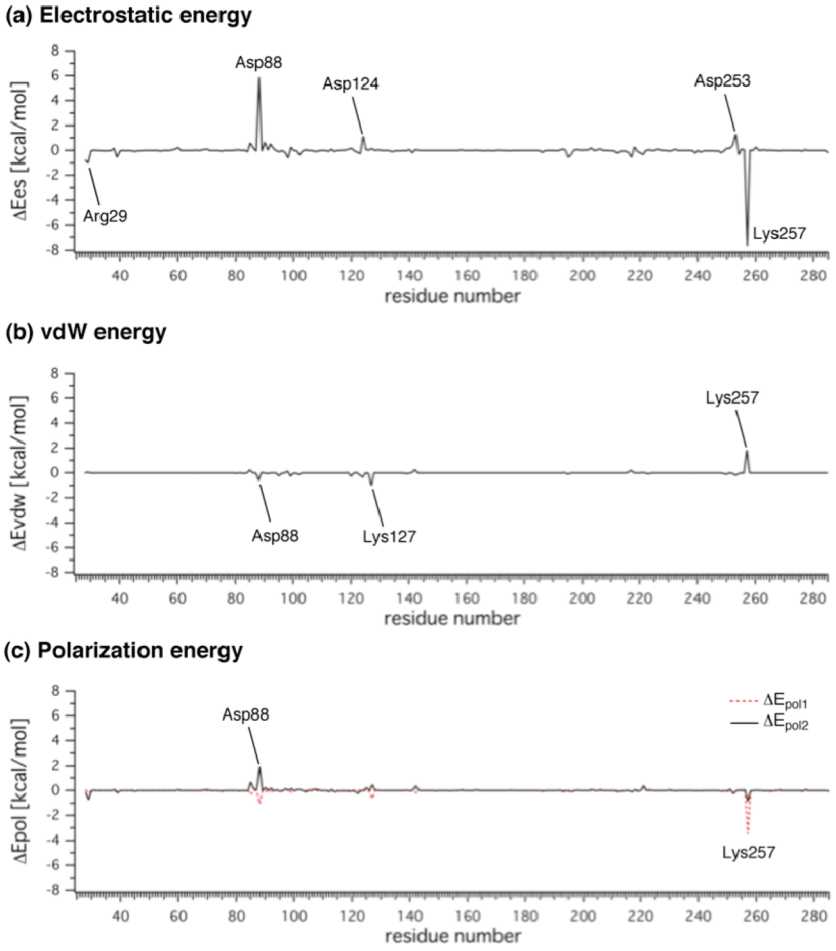

Figure 3. Residue contributions to the interaction energy terms: (a) electrostatic energy (b) vdW energy, and (c) polarization energy.

Table 5. Ten Largest Pairwise Dispersion Energy Terms Between the O_2 Molecule (O_a and O_b) and the Surrounding Atoms Obtained for the ONIOM(D′)-EE Geometry[a]

for O_a		for O_b	
atom	dispersion energy (kcal/mol)	atom	dispersion energy (kcal/mol)
C1 (MI)	−0.305	N_ε (His98)	−0.296
N_ε (His98)	−0.295	O_x	−0.255
H1 (MI)	−0.259	$O_{\delta 1}$ (Asp253)	−0.252
$O_{\delta 2}$ (Asp124)	−0.255	C1 (MI)	−0.241
O1 (MI)	−0.250	H1 (MI)	−0.207
Fe2	−0.234	C_ε (His98)	−0.186
O_x	−0.220	Fe2	−0.147
C_δ (His98)	−0.203	C_γ (Asp253)	−0.107
C2 (MI)	−0.152	O1 (MI)	−0.101
H2 (MI)	−0.131	C_δ (His98)	−0.084

[a] Energies calculated with an s_6 value of 1.05 are presented.

(1.9 kcal/mol). The value for a nearby water molecule (w4) was −0.7 kcal/mol. Therefore, although the vdW effect stabilizes the O_2-bound state by 2.2 kcal/mol (Table 4), this is because of the accumulation of small contributions from the residues. As for the polarization effect, E^k_{pol1} or E^k_{pol2} provided qualitatively different trends for Asp88. It was found that E^k_{pol1} for Asp88 had a stabilizing effect (−1.0 kcal/mol), whereas E^k_{pol2} had a destabilizing effect (+2.0 kcal/mol). For Lys257, E^k_{pol1} was −3.5 kcal/mol, while E^k_{pol2} was −0.8 kcal/mol. In any case, the total polarization stabilization is only 0.7 kcal/mol (Table 4) and the contribution of each residue is only marginal.

The dispersion energy formula (eq 3) allows one to analyze pairwise atom−atom dispersion energy contributions. Table 5 lists atom pairs that have relatively large dispersion interaction energies with the oxygen atoms in the O_2 molecule. It can be seen that for both O_a and O_b, the dispersion stabilization due to the interaction with Fe1 is not large (−0.042 kcal/mol for O_a and −0.036 kcal/mol for O_b). The interaction with Fe2 is larger: the dispersion energies were −0.234 kcal/mol for O_a and −0.147 kcal/mol for O_b. The dispersion stabilization due to the interaction with the MI ligand was also relatively large, especially with C1 and the abstracted hydrogen (H1). The coordinating nitrogen atom (N_ε) of His98 and its neighbors interact relatively strongly. Other atoms coordinating to Fe1 also have relatively large stabilization energies due to dispersion. In summary, the ferric-superoxide formation in MIOX is facilitated by the interaction between O_2 and ligands around the iron, to which O_2 is eventually bound, as well as the MI substrate.

4. CONCLUSION

We have performed a combined ONIOM(DFT(-D):MM) and energy decomposition analysis to clarify the effects of the

protein environment and dispersion on one of the key steps in the catalytic cycle of MIOX, namely O_2 binding to a ferrous center to produce a ferric-superoxide intermediate. Our analysis shows that the electrostatic, vdW, and polarization interactions enhance O_2 binding in MIOX, but their contributions are relatively small. The major part of the O_2 binding energy originates from the stabilization of the O_2-bound state due to dispersion interactions between the O_2 unit and the atoms in the active-site cluster. Some of the atoms in the MI substrate also have relatively large dispersion stabilization effects. The energy decomposition analysis presented in this study should also further our understanding of other complex biological systems, which hopefully facilitates the rational design of bioinspired catalysts in the future.

■ ASSOCIATED CONTENT

Supporting Information. Full ref 24, raw energy data, and XYZ coordinates of QM atoms. This material is available free of charge via the Internet at http://pubs.acs.org.

■ AUTHOR INFORMATION

Corresponding Author
*E-mail: hirao@ntu.edu.sg.

■ ACKNOWLEDGMENT

H.H. thanks Nanyang Assistant Professorship for financial support and The High Performance Computing Centre (HPCC) at Nanyang Technological University for computer resources. This paper is dedicated to Prof. Keiji Morokuma on the occasion of his 77th birthday.

■ REFERENCES

(1) (a) Warshel, A.; Sharma, P. K.; Kato, M.; Xiang, Y.; Liu, H.; Olsson, M. H. M. *Chem. Rev.* **2006**, *106*, 3210–3235. (b) Senn, H. M.; Thiel, W. *Curr. Opin. Chem. Biol.* **2007**, *11*, 182–187. (c) Shaik, S.; Cohen, S.; Wang, Y.; Chen, H.; Kumar, D.; Thiel, W. *Chem. Rev.* **2010**, *110*, 949–1017. (d) Acevedo, O.; Jorgensen, W. L. *Acc. Chem. Res.* **2010**, *43*, 142–151. (e) Ranaghan, K. E.; Mulholland, A. J. *Int. Rev. Phys. Chem.* **2010**, *29*, 65–133. (f) Riccardi, D.; Yang, S.; Cui, Q. *Biochim. Biophys. Acta* **2010**, *1804*, 342–351.

(2) (a) Costas, M.; Mehn, M. P.; Jensen, M. P.; Que, L., Jr. *Chem. Rev.* **2004**, *104*, 939–986. (b) Que, L., Jr.; Tolman, W. B. *Nature* **2008**, *455*, 333–340. (c) Mukherjee, A.; Cranswick, M. A.; Chakrabarti, M.; Paine, T. K.; Fujisawa, K.; Munck, E.; Que, L., Jr. *Inorg. Chem.* **2010**, *49*, 3618–3628. (d) Nam, W. *Acc. Chem. Res.* **2007**, *40*, 522–531.

(3) (a) Ogo, S. *Dalton Trans.* **2010**, *39*, 2963–2963 and articles in that issue. (b) Chaudhuri, P.; Wieghardt, K.; Weyhermüller, T.; Paine, T. K.; Mukherjee, S.; Mukherjee, C. *Biol. Chem.* **2005**, *386*, 1023–1033.

(4) Deuss, P. J.; den Heeten, R.; Laan, W.; Kamer, P. C. J. *Chem.—Eur. J.* **2011**, *17*, 4680–4698.

(5) For recent reviews on QM/MM methods for the studies of enzymes, see for example (a) Friesner, R. A.; Guallar, V. *Annu. Rev. Phys. Chem.* **2005**, *56*, 389–427. (b) Senn, H. M.; Thiel, W. *Top. Curr. Chem.* **2007**, *268*, 173–290. (c) Senn, H. M.; Thiel, W. *Angew. Chem., Int. Ed.* **2009**, *48*, 1198–1229. (d) Hu, H.; Yang, W. *J. Mol. Struct.: THEOCHEM* **2009**, *898*, 17–30. (e) Zhang, R.; Lev, B.; Cuervo, J. E.; Noskov, S. Y.; Salahub, D. R. *Adv. Quantum Chem.* **2010**, *59*, 353–400.

(6) (a) Maseras, F.; Morokuma, K. *J. Comput. Chem.* **1995**, *16*, 1170–1179. (b) Svensson, M.; Humbel, S.; Froese, R. D. J.; Matsubara, T.; Sieber, S.; Morokuma, K. *J. Phys. Chem.* **1996**, *100*, 19357–19363. (c) Vreven, T.; Morokuma, K.; Farkas, Ö.; Schlegel, H. B.; Frisch, M. J. *J. Comput. Chem.* **2003**, *24*, 760–769. (d) Vreven, T.; Byun, K. S.; Komáromi, I.; Dapprich, S.; Montgomery, J. A., Jr.; Morokuma, K.; Frisch, M. J. *J. Chem. Theory Comput.* **2006**, *2*, 815–826.

(7) (a) Xing, G.; Hoffart, L. M.; Diao, Y.; Prabhu, K. S.; Arner, R. J.; Reddy, C. C.; Krebs, C.; Bollinger, J. M., Jr. *Biochemistry* **2006**, *45*, 5393–5401. (b) Xing, G.; Barr, E. W.; Diao, Y.; Hoffart, L. M.; Prabhu, K. S.; Arner, R. J.; Reddy, C. C.; Krebs, C.; Bollinger, J. M., Jr. *Biochemistry* **2006**, *45*, 5402–5412. (c) Xing, G.; Diao, Y.; Hoffart, L. M.; Barr, E. W.; Prabhu, K. S.; Arner, R. J.; Reddy, C. C.; Krebs, C.; Bollinger, J. M., Jr. *Proc. Natl. Acad. Sci. U.S.A.* **2006**, *103*, 6130–6135. (d) Bollinger, J. M., Jr.; Diao, Y.; Matthews, M. L.; Xing, G.; Krebs, C. *Dalton Trans.* **2009**, *No. 6*, 905–914.

(8) (a) Brown, P. M.; Caradoc-Davies, T. T.; Dickson, J. M. J.; Cooper, G. J. S.; Loomes, K. M.; Baker, E. N. *Proc. Natl. Acad. Sci. U.S.A.* **2006**, *103*, 15032–15037. (b) Thorsell, A. G.; Persson, C.; Voevodskaya, N.; Busam, R. D.; Hammarström, M.; Gräslund, S.; Gräslund, A.; Hallberg, B. M. *J. Biol. Chem.* **2008**, *283*, 15209–15216.

(9) (a) Bollinger., J. M., Jr.; Krebs, C. *Curr. Opin. Chem. Biol.* **2007**, *11*, 151–158. (b) van der Donk, W. A.; Krebs, C.; Bollinger, J. M., Jr. *Curr. Opin. Struct. Biol.* **2010**, *20*, 673–683. (c) Kovaleva, E. G.; Lipscomb, J. D. *Nat. Chem. Biol.* **2008**, *4*, 186–193.

(10) Hirao, H.; Morokuma, K. *J. Am. Chem. Soc.* **2009**, *131*, 17206–17214.

(11) Bassan, A.; Blomberg, M. R. A.; Siegbahn, P. E. M. *Chem.—Eur. J.* **2003**, *9*, 106–115.

(12) (a) Schenk, G.; Pau, M. Y. M.; Solomon, E. I. *J. Am. Chem. Soc.* **2004**, *126*, 505–515. (b) Davis, M. I.; Wasinger, E. C.; Decker, A.; Pau, M. Y. M.; Vaillancourt, F. H.; Bolin, J. T.; Eltis, L. D.; Hedman, B.; Hodgson, K. O.; Solomon, E. I. *J. Am. Chem. Soc.* **2003**, *125*, 11214–11227. (c) Brown, C. D.; Neidig, M. L.; Neibergall, M. B.; Lipscomb, J. D.; Solomon, E. I. *J. Am. Chem. Soc.* **2007**, *129*, 7427–7438.

(13) Wirstam, M.; Lippard, S. J.; Friesner, R. A. *J. Am. Chem. Soc.* **2003**, *125*, 3980–3987.

(14) Hoffman, M.; Khavrutskii, I. V.; Musaev, D. G.; Morokuma, K. *Int. J. Quantum Chem.* **2004**, *99*, 972–980.

(15) Nemukhin, A. V.; Grigorenko, B. L.; Topol., I. A.; Burt, S. K. *Int. J. Quantum Chem.* **2006**, *106*, 2184–2190.

(16) Lundberg, M.; Morokuma, K. *J. Phys. Chem. B* **2007**, *111*, 9380–9389.

(17) (a) Kitaura, K.; Morokuma, K. *Int. J. Quantum Chem.* **1976**, *10*, 325–340. (b) Curutchet, C.; Bofill, J. M.; Hernández, B.; Orozco, M.; Luque, F. J. *J. Comput. Chem.* **2003**, *24*, 1263–1275. (c) Mo, Y.; Gao, J. *J. Phys. Chem. B* **2006**, *110*, 2976–2980.

(18) (a) Hayashi, S.; Ohmine, I. *J. Phys. Chem. B* **2000**, *104*, 10678–10691. (b) Ishida, T. *J. Chem. Phys.* **2008**, *129*, 125105/1–125105/14. (c) Fedorov, D. G.; Kitaura, K. *J. Phys. Chem. A* **2007**, *111*, 6904–6914.

(19) Grimme, S. *J. Comput. Chem.* **2006**, *27*, 1787–1799.

(20) Neese, F.; Liakos, D. G.; Ye, S. *J. Biol. Inorg. Chem.* **2011**, *16*, 821–829.

(21) Hirao, H.; Morokuma, K. *J. Phys. Chem. Lett.* **2010**, *1*, 901–906.

(22) Siegbahn, P. E. M.; Blomberg, M. R. A.; Chen, S. L. *J. Chem. Theory Comput.* **2010**, *6*, 2040–2044.

(23) Lonsdale, R.; Harvey, J. N.; Mulholland, A. J. *J. Phys. Chem. Lett.* **2010**, *1*, 3232–3237.

(24) Frisch, M. J.; Trucks, G. W.; Schlegel, H. B.; Scuseria, G. E.; Robb, M. A.; Cheeseman, J. R.; Montgomery, J. A., Jr.; Vreven, T.; Kudin, K.; Burant, J. C. et al. *Gaussian 09*, revision B.01; Gaussian, Inc.: Wallingford, CT, 2010.

(25) (a) Becke, A. D. *J. Chem. Phys.* **1993**, *98*, 5648–5652. (b) Lee, C.; Yang, W.; Parr, R. G. *Phys. Rev. B* **1988**, *37*, 785–789. (c) Vosko, S. H.; Wilk, L.; Nusair, M. *Can. J. Phys.* **1980**, *58*, 1200–1211.

(26) (a) Dolg, M.; Wedig, U.; Stoll, H.; Preuss, H. *J. Chem. Phys.* **1987**, *86*, 866–872.(b) Hehre, W.; Radom, L.; Schleyer, P. v. R.; Pople, J. *Ab Initio Molecular Orbital Theory*; John Wiley & Sons: New York, 1986.

(27) Cornell, W. D.; Cieplak, P.; Bayly, C. I.; Gould, I. R.; Merz, K. M., Jr.; Ferguson, D. M.; Spellmeyer, D. C.; Fox, T.; Caldwell, J. W.; Kollman, P. A. *J. Am. Chem. Soc.* **1995**, *117*, 5179–5197.

(28) Jorgensen, W. L.; Chandrasekhar, J.; Madura, J. D.; Impey, R. W.; Klein, M. L. *J. Chem. Phys.* **1983**, *79*, 926–935.
(29) (a) Singh, U. C.; Kollman, P. A. *J. Comput. Chem.* **1984**, *5*, 129–145. (b) Besler, B. H.; Merz, K. M.; Kollman, P. A. *J. Comput. Chem.* **1990**, *11*, 431–439.
(30) Humphrey, W.; Dalke, A.; Schulten, K. *J. Mol. Graphics* **1996**, *14*, 33–38.
(31) Reiher, M.; Salomon, O.; Hess, B. A. *Theor. Chem. Acc.* **2001**, *107*, 48–55.
(32) Siegbahn, P. E. M. *J. Biol. Inorg. Chem.* **2006**, *11*, 695–701.